

## Molecular-dynamics calculations of energetics and geometries of steps on diamond C(001)

M.-H. Tsai and Y.-Y. Yeh

*Department of Physics, National Sun Yat-Sen University, Kaohsiung, Taiwan 804, Republic of China*

(Received 13 March 1997; revised manuscript received 20 October 1997)

The diamond C(001) surface has been observed by scanning tunneling microscopy (STM) to dimerize similar to Si(001). STM also observed the formation of single- and double-layer steps in this surface. Using an *ab initio* multicenter molecular-dynamics method, our calculations for the relaxed geometries and the corresponding energetics of these steps show that the detailed structures of these steps are intrinsically different from that of type-A and type-B steps of Si(001) obtained by Chadi. These differences can be attributed to the preference of carbon atoms near the edges of the lower terrace to form dimers with strong mixed single and double bonds rather than to rebond to the edge atoms. [S0163-1829(98)05127-3]

Studies of homoepitaxial diamond films by chemical vapor deposition have recently been made toward the growth of high-quality single-crystalline diamond films and the understanding of growth mechanism. Morphological studies using scanning tunneling microscopy (STM) and low-energy electron diffraction have found  $(2 \times 1)$  reconstruction and single-layer steps on the homoepitaxial diamond C(001) films.<sup>1-7</sup> Double-layer steps with step edges parallel to the dimer rows have also been observed in coexistence with single-layer steps when the diamond (001) surface was annealed in hydrogen plasma.<sup>6-10</sup> Following Chadi,<sup>11</sup> we shall denote single-layer steps  $S_A$  and  $S_B$  and double-layer steps  $D_A$  and  $D_B$  as the steps with step edges that run parallel and perpendicular to the dimer rows on the upper terraces, respectively. STM measurements found that step edges of  $S_A$  were almost straight, whereas those of  $S_B$  were ragged with many kinks. These observations suggested that  $S_A$  steps have a formation energy lower than that of  $S_B$  similar to Si(001) grown by molecular beam epitaxy. The occurrence of  $D_A$  steps and the absence of  $D_B$  steps in STM observations suggested that the formation energy of the  $D_A$  step is lower than that of the  $D_B$  step in contrast to Si(001), which led Kuang *et al.*<sup>10</sup> to suggest that the saturation of dangling bonds by hydrogen atoms present in the experimental environment might reverse the preference of  $D_B$ .

To understand these STM observations, we have carried out this study using the *ab initio* multicenter molecular dynamics (MD) method of Sankey and Niklewski.<sup>12</sup> This method is based on the norm-conserving pseudopotential method<sup>13,14</sup> with  $s$ ,  $p_x$ ,  $p_y$ , and  $p_z$  local-orbital basis set and has been shown to work well for semiconductor systems<sup>15-18</sup> and diamond.<sup>19</sup> The theoretical lattice constant of 3.7 Å (about 3.7% error from the experimental value<sup>20</sup> of 3.567 Å) determined by bulk diamond calculations using a cubic unit cell and repeated five- and six-layer slab (or supercell) models are used for  $S_A$  and  $S_B$  steps. For  $D_A$  and  $D_B$  steps, only repeated six-layer-slab models are used. The need for choosing both five- and six-layer supercell models for  $S_A$  and  $S_B$  steps will be described later. We have chosen a  $(11 \times 2)$  unit cell for all steps. For  $S_A$  and  $S_B$  steps, twelve surface atoms per unit cell form the upper terrace and the exposed second-layer atoms form the lower terrace. For the  $D_A$  step, 12 surface atoms per unit cell are chosen to form the upper terrace.

However, ten surface atoms per unit cell are chosen for  $D_B$  in order to have the same geometry on both edges. Twelve and sixteen atoms per unit cell are chosen, respectively, for  $D_A$  and  $D_B$  steps for the second layer, i.e., the layer beneath the upper terrace. The exposed third-layer atoms form the lower terrace for  $D_A$  and  $D_B$  steps. These models have been chosen by analogy with that of Chadi.<sup>11</sup> Since the rebonding edge atoms in the second layer of  $D_B$  are not covered or bonded to surface atoms, we have considered a  $D'_B$  step with a sharper edge, in which the second layer contains only twelve atoms per unit cell. We have also considered  $S'_B$  and  $D'_A$  steps, which have different dimer arrangements on the lower terrace of  $S_B$  and  $D_B$  steps, respectively, to be shown later. Calculations of the relaxed geometry and total energy of the  $(2 \times 1)$  reconstructed surface with the same  $(11 \times 2)$  unit cell using a five-layer repeated slab model have also been performed. The formation energy of this  $(2 \times 1)$  surface is used as a reference to determine the formation energies of  $S_A$ ,  $S_B$ ,  $S'_B$ ,  $D_A$ ,  $D'_A$ ,  $D_B$ , and  $D'_B$  steps. For all models, the atoms of the bottom layer and the layer above are assigned an arbitrarily large mass so that they are essentially motionless and each bottom-layer atom is attached with two artificial H atoms in the dangling-bond directions to saturate its two dangling bonds to simulate bulk atoms. We start the MD calculations with the dimerized surface on both upper

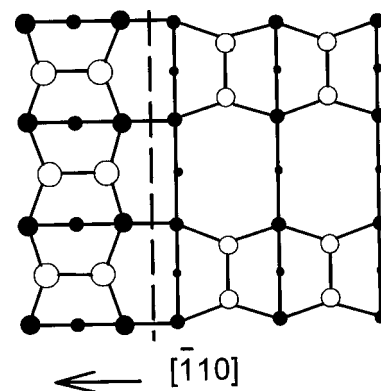


FIG. 1. Top view of the  $S_A$  step. The sizes of circles are in descending order from the topmost layer to inner layers. Atoms represented by open circles have dangling bonds.

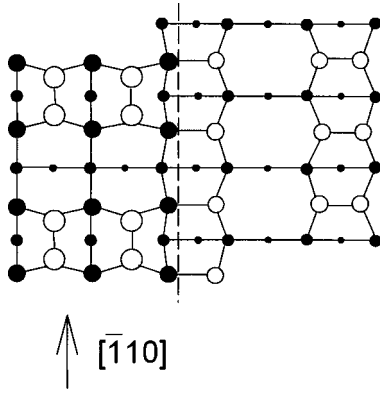


FIG. 2. Top view of the  $S_B$  step. The sizes of circles are in descending order from the topmost layer to inner layers. Atoms represented by open circles have dangling bonds.

and lower terraces and sample only the  $\bar{\Gamma}$  point. The Newtonian equations of motion are solved numerically for a time step of 0.62 fs using the fifth-order Gear algorithm.<sup>21</sup> We use a quenching scheme,<sup>15</sup> not the simulated annealing, to let atoms settle to their stable or metastable positions with the criterion that the force acting on each atom is less than 0.1 eV/Å. After the stable or metastable atomic positions are found, we sample four and sixteen special  $\mathbf{k}$  points in the irreducible Brillouin zone for a two-dimensional rectangular lattice<sup>22</sup> to calculate the total energies. Both yield essentially the same total energies per atom within 0.5 meV. Thus, the total energies are well converged with respect to the number of  $\mathbf{k}$  points.

The top views of the relaxed geometries for  $S_A$ ,  $S_B$ ,  $S'_B$ ,  $D_A$ ,  $D'_A$ ,  $D_B$ , and  $D'_B$  steps are shown in Figs. 1–7, respectively. They are drawn by analogy with that of Chadi,<sup>11</sup> so that the differences between diamond and silicon can be easily seen. The average dimer bond lengths for  $S_A$  are 1.457 and 1.405 Å for the upper and lower terraces, respectively. For  $S_B$ , they are 1.437 and 1.538 Å. For  $S'_B$ , they are 1.451 and 1.493 Å. For  $D_A$ , they are 1.494 and 1.511 Å. For  $D'_A$ , they are 1.427 and 1.479 Å. For  $D_B$ , they are 1.398 and 1.409 Å. And for  $D'_B$ , they are 1.434 and 1.402 Å. The total energies per atom, which include the binding energies with the artificial H atoms used for saturating the dangling bonds of bottom-layer atoms, are  $-156.2833$ ,  $-156.3572$ ,  $-156.2022$ ,  $-156.3203$ ,  $-156.1742$ ,  $-156.3434$ ,

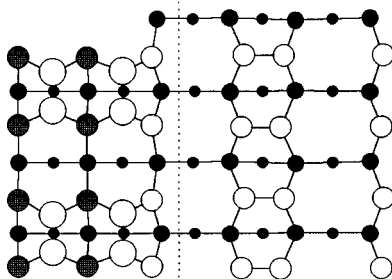


FIG. 3. Top view of the  $S'_B$  step. The sizes of circles are in descending order from the topmost layer to inner layers. Atoms represented by open circles have dangling bonds.

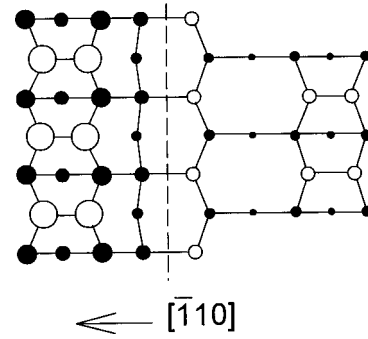


FIG. 4. Top view of the  $D_A$  step. The sizes of circles are in descending order from the topmost layer to inner layers. Atoms represented by open circles have dangling bonds.

$-156.1986$ ,  $-156.2215$ ,  $-156.2354$ ,  $-156.2330$ , and  $-156.2753$  eV, respectively, for the  $(2 \times 1)$  surface,  $S_A(5l)$ ,  $S_A(6l)$ ,  $S_B(5l)$ ,  $S_B(6l)$ ,  $S'_B(5l)$ ,  $S'_B(6l)$ ,  $D_A$ ,  $D'_A$ ,  $D_B$ , and  $D'_B$  steps, where  $5l$  and  $6l$  stand for five- and six-layer slab models. The density and bonding arrangements of the artificial H atoms are the same in all the step models and the  $(2 \times 1)$  surface, as are the binding energies with bottom-layer C atoms, so that they can be canceled out in the comparison between energies. If  $E_{\text{tot}}^s$ ,  $E_{\text{tot}}^{2 \times 1}$ , and  $E_{\text{bulk}}$  are the total energies per atom for the step,  $(2 \times 1)$  surface, and bulk diamond crystal, respectively, and  $n_s$  and  $n_{2 \times 1}$  are the numbers of C atoms in the unit cell for the step and  $(2 \times 1)$  surface, respectively, the formation energy per step unit length,  $\lambda$  is calculated as

$$\lambda = [(E_{\text{tot}}^s - E_{\text{bulk}})n_s - (E_{\text{tot}}^{2 \times 1} - E_{\text{bulk}})n_{2 \times 1}]/4, \quad (1)$$

or

$$\lambda = [E_{\text{tot}}^s n_s - E_{\text{tot}}^{2 \times 1} n_{2 \times 1} - E_{\text{bulk}}(n_s - n_{2 \times 1})]/4, \quad (2)$$

since  $E_{\text{bulk}}$  is the chemical potential energy of these systems. The factor 4 in Eqs. (1) and (2) is due to the fact that there are two step edges and two unit lengths per unit cell in our models.  $n_{2 \times 1} = 132$  and  $n_s$ 's are 122, 144, 122, 144, 122, 144, 134, 134, 136, and 132 for  $S_A(5l)$ ,  $S_A(6l)$ ,  $S_B(5l)$ ,  $S_B(6l)$ ,  $S'_B(5l)$ ,  $S'_B(6l)$ ,  $D_A$ ,  $D'_A$ ,  $D_B$ , and  $D'_B$  steps, respectively. To reduce possible systematic errors due to  $E_{\text{bulk}}$ , which is calculated with a different unit cell,  $|n_s - n_{2 \times 1}|$  should be as small as possible as indicated in Eq. (2). Thus, we need to consider both five- and six-layer supercell models

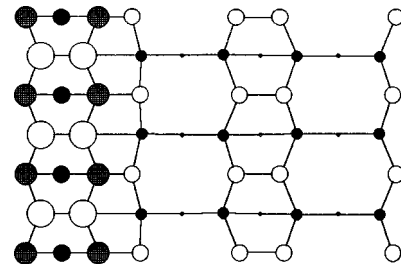


FIG. 5. Top view of the  $D'_A$  step. The sizes of circles are in descending order from the topmost layer to inner layers. Atoms represented by open circles have dangling bonds.

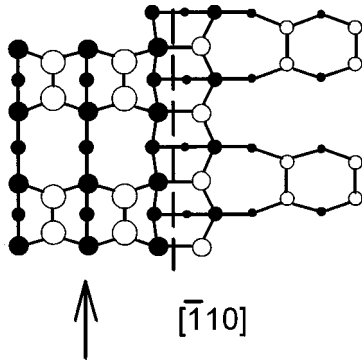


FIG. 6. Top view of the  $D_B$  step. The sizes of circles are in descending order from the topmost layer to inner layers. Atoms represented by open circles have dangling bonds.

for  $S_A$ ,  $S_B$ , and  $S'_B$  steps so that their average  $n_s$ , i.e., 133, is close to  $n_{2 \times 1}$ .  $E_{\text{bulk}}$  is determined with the four special  $\mathbf{k}$  points of Chadi and Cohen<sup>23</sup> for a simple cubic lattice to be  $-155.2960$  eV. The formation energies per unit step length for  $S_A$ ,  $S_B$ ,  $S'_B$ ,  $D_A$ ,  $D'_A$ ,  $D_B$ , and  $D'_B$  steps are given in Table I. Here, the formation energies for  $S_A$ ,  $S_B$ , and  $S'_B$  are the averages of those of five- and six-layer supercell models.

The formation energy of  $S_A$  is smaller than that of  $S_B$  or  $S'_B$  in agreement with STM observations. All the formation energies of  $S_A$ ,  $D_A$ , and  $D_B$  steps, which are considered by analogy with those of Chadi<sup>11</sup> for Si(001), are larger than those of their alternative  $S'_B$ ,  $D'_A$ , and  $D'_B$  steps. In other words,  $S'_B$ ,  $D'_A$ , and  $D'_B$  steps are more favorable than  $S_B$ ,  $D_A$ , and  $D_B$  steps, respectively. These results show that the structural properties of diamond C(001) are intrinsically different from those of Si(001). The formation energies of  $D_B$  and  $D'_B$  are smaller than those of  $D_A$  and  $D'_A$ , which are similar to Si(001) and do not agree with STM observations. Since STM measurements were done after annealing in the hydrogen environment, Kuang *et al.*<sup>10</sup> thought that STM observations of  $D_A/D'_A$  rather than  $D_B/D'_B$  were due to the saturation of C dangling bonds by hydrogen atoms. To understand if this was the case, we have calculated the relaxed geometries and total energies of  $D_A$ ,  $D'_A$ ,  $D_B$ , and  $D'_B$  by saturating their dangling bonds with real hydrogen atoms, whose energy level and coupling constants have been determined by a more elaborate self-consistent-charge-density method.<sup>24</sup> By assuming that the carbon dimer has a single bond, both  $D_A$  and  $D_B$  have 20 dangling bonds, while both

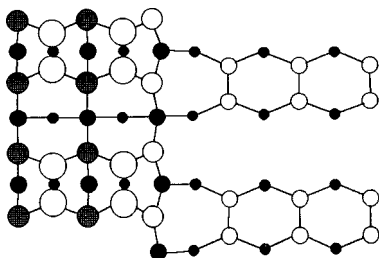


FIG. 7. Top view of the  $D'_B$  step. The sizes of circles are in descending order from the topmost layer to inner layers. Atoms represented by open circles have dangling bonds.

TABLE I. Formation energies in eV per unit step length for the steps  $S_A$ ,  $S_B$ ,  $S'_B$ ,  $D_A$ ,  $D'_A$ ,  $D_B$ , and  $D'_B$ .

$S_A$	$S_B$	$S'_B$	$D_A$	$D'_A$	$D_B$	$D'_B$
0.13	1.15	0.36	1.58	1.11	0.72	0.26

$D'_A$  and  $D'_B$  have 24 dangling bonds per unit cell to be saturated by hydrogen atoms. The saturation of these dangling bonds increases the dimer bond length to  $1.58$  Å, which is close to the experimental value for the single bond of  $1.54$  Å.<sup>20</sup> The total energies per atoms for  $D'_A$  ( $D_A$ ) and  $D'_B$  ( $D_B$ ) are then  $-157.3467$  ( $-157.1436$ ) and  $-157.3229$  ( $-157.1206$ ) eV, respectively. The type-A step becomes lower in energy, which supports the view of Kuang *et al.*<sup>10</sup>

The lower formation energy for  $S_A$  than for  $S_B$ ,  $D_A$ , and  $D_B$  has been explained by Chadi for Si(001) in that it is the step that does not lead to large strain or to extra dangling bonds. The same is true for diamond C(001) even compared to  $S'_B$ ,  $D'_A$ , and  $D'_B$ .  $S'_B$  and  $D'_A$  differ from  $S_B$  and  $D_A$  by the displacement of rebonded edge atoms on the lower terrace to form dimers with neighboring atoms on the lower terrace as shown in Figs. 2–5. And  $D'_B$  differs from  $D_B$  by the removing of rebonded edge atoms in the second layer so that the new exposed atoms on the lower terrace can form extra dimers as shown in Figs. 6 and 7. The rebonded edge atoms have only single bonds, while the C dimer may have a double bond or a hybridization of single and double bonds, which significantly reduces the effective number of dangling bonds. The results that  $S'_B$ ,  $D'_A$ , and  $D'_B$  are more favorable than  $S_B$ ,  $D_A$ , and  $D_B$ , respectively, show that dimerization is more effective in reducing dangling bonds than rebonding for diamond. The formation of the double bond or hybridization of single and double bonds is a unique property of carbon as evidenced by its formation of the benzene structure, which does not occur naturally for Si. The calculated dimer bond lengths are ranged between  $1.398$  and  $1.538$  Å, which are between that of the single bond of  $1.54$  Å and the double bond of  $1.34$  Å.<sup>20</sup> These bond length results show that the dimer bond is a hybridization of single and double bonds. The hydrogen induced elongation of the dimer further supports this argument.

In summary, our MD calculations for diamond C(001) show that the geometries of the single-layer type-B step and double-layer type-A and type-B steps are intrinsically different from that of Si(001) given by Chadi. These differences can be attributed to the unique property of carbon atoms to hybridize single and double bonds, which renders the rebonding of atoms near the edge less favorable than forming dimers. The results that the saturation of dangling bonds by hydrogen atoms reverses the order of formation energies of double-layer type-A and type-B steps support the explanation of Kuang *et al.* of their STM observation of type-A, not type-B, steps.

We are grateful to Dr. T. T. Tsong of the Institute of Physics, Academia Sinica, for suggesting this study, and to the National Science Council of the Republic of China for its generous support (Contract No. NSC86-2112-M-110-002).

- <sup>1</sup>H. Kawarada, M. Aoki, H. Sasaki, and K. Tsugawa, *Diamond Relat. Mater.* **3**, 961 (1994).
- <sup>2</sup>H. G. Maguire, M. Kamo, H. P. Lang, and H.-J. Güntherodt, *Appl. Surf. Sci.* **75**, 144 (1994).
- <sup>3</sup>Th. Frauenheim, U. Stephan, P. Blaudeck, D. Porezag, H.-G. Bugmann, and W. Zimmermann-Edling, *Diamond Relat. Mater.* **3**, 966 (1994).
- <sup>4</sup>R. E. Stallcup, A. F. Aviles, and J. M. Perez, *Appl. Phys. Lett.* **66**, 2331 (1995).
- <sup>5</sup>Y. Kuang, N. Lee, A. Badzian, T. T. Tsong, T. Badzian, and C. Chen, *Diamond Relat. Mater.* **4**, 1371 (1995).
- <sup>6</sup>N. Lee and A. Badzian (unpublished).
- <sup>7</sup>T. Tsuno, T. Imai, Y. Nishibayashi, K. Hamada, and N. Fujimori, *Jpn. J. Appl. Phys., Part 1* **30**, 1063 (1991).
- <sup>8</sup>T. Tsuno, T. Tomikawa, S. Shikata, T. Imai, and N. Fujimori, *Appl. Phys. Lett.* **64**, 572 (1994).
- <sup>9</sup>M. A. Tamor and M. P. Everson, *J. Mater. Res.* **8**, 1770 (1993).
- <sup>10</sup>Y. Kuang, Y. Wang, N. Lee, A. Badzian, T. Badzian, and T. T. Tsong, *Appl. Phys. Lett.* **67**, 3721 (1995).
- <sup>11</sup>D. J. Chadi, *Phys. Rev. Lett.* **59**, 1691 (1987).
- <sup>12</sup>O. F. Sankey and D. J. Niklewski, *Phys. Rev. B* **40**, 3979 (1989).
- <sup>13</sup>D. R. Hamann, M. Schlüter, and C. Chiang, *Phys. Rev. Lett.* **43**, 1494 (1979).
- <sup>14</sup>G. B. Bachelet, D. R. Hamann, and M. Schlüter, *Phys. Rev. B* **26**, 4199 (1982).
- <sup>15</sup>G. B. Adams and O. F. Sankey, *Phys. Rev. Lett.* **67**, 867 (1991).
- <sup>16</sup>D. A. Drabold, P. A. Fedders, S. Klemm, and O. F. Sankey, *Phys. Rev. Lett.* **67**, 2179 (1991).
- <sup>17</sup>D. A. Drabold, P. A. Fedders, and P. Stumm, *Phys. Rev. B* **49**, 16 415 (1994).
- <sup>18</sup>H. Feil, H. J. W. Zandvliet, M.-H. Tsai, J. D. Dow, and I. S. T. Tsong, *Phys. Rev. Lett.* **69**, 3076 (1992).
- <sup>19</sup>S. H. Yang, D. A. Drabold, and J. B. Adams, *Phys. Rev. B* **48**, 5261 (1993).
- <sup>20</sup>*CRC Handbook of Chemistry and Physics*, 73rd ed., edited by David R. Lide (CRC, Boca Raton, FL, 1992).
- <sup>21</sup>C. W. Gear (unpublished).
- <sup>22</sup>S. L. Cunningham, *Phys. Rev. B* **10**, 4988 (1974).
- <sup>23</sup>D. J. Chadi and M. L. Cohen, *Phys. Rev. B* **8**, 5747 (1973).
- <sup>24</sup>M.-H. Tsai and K. C. Hass, *Phys. Rev. B* **52**, 16 420 (1995).